



# The Ragulator complex serves as a substrate-specific mTORC1 scaffold in regulating the nuclear translocation of transcription factor EB

Received for publication, August 27, 2021, and in revised form, January 31, 2022. Published, Papers in Press, February 18, 2022.

<https://doi.org/10.1016/j.jbc.2022.101744>

Tetsuya Kimura<sup>1,\*</sup>, Yoshitomo Hayama<sup>2</sup>, Daisuke Okuzaki<sup>3,4,5</sup>, Shigeyuki Nada<sup>1,6</sup> , and Masato Okada<sup>1,6</sup>

From the <sup>1</sup>Department of Oncogene Research, WPI Immunology Frontier Research Center, <sup>2</sup>Department of Respiratory Medicine and Clinical Immunology, Graduate School of Medicine, <sup>3</sup>Single Cell Genomics, Human Immunology, WPI Immunology Frontier Research Center, <sup>4</sup>Genome Information Research Center, Research Institute for Microbial Diseases, <sup>5</sup>Institute for Open and Transdisciplinary Research Initiatives, and <sup>6</sup>Department of Oncogene Research, Research Institute for Microbial Diseases, Osaka University, Suita, Osaka, Japan

Edited by Phyllis Hanson

The mammalian target of rapamycin complex 1 (mTORC1) signaling pathway is activated by intracellular nutritional sufficiency and extracellular growth signals. It has been reported that mTORC1 acts as a hub that integrates these inputs to orchestrate a number of cellular responses, including translation, nucleotide synthesis, lipid synthesis, and lysosome biogenesis. However, little is known about specific control of mTORC1 signaling downstream of this complex. Here, we demonstrate that Ragulator, a heteropentameric protein complex required for mTORC1 activation in response to amino acids, is critical for inhibiting the nuclear translocation of transcription factor EB (TFEB). We established a unique RAW264.7 clone that lacked Ragulator but retained total mTORC1 activity. In a nutrition-sufficient state, the nuclear translocation of TFEB was markedly enhanced in the clone despite total mTORC1 kinase activity. In addition, as a cellular phenotype, the number of lysosomes was increased by tenfold in the Ragulator-deficient clone compared with that of control cells. These findings indicate that mTORC1 essentially requires the Ragulator complex for regulating the subcellular distribution of TFEB. Our findings also suggest that other scaffold proteins may be associated with mTORC1 for the specific regulation of downstream signaling.

mTORC1 is a kinase complex that integrates nutritional sufficiency and growth hormone signals as inputs. Several studies have reported that mTORC1 orchestrates multiple cellular responses, including translation (1), organelle biogenesis (1), lipid synthesis (2), and nucleotide synthesis (3, 4). mTORC1 is implicated in numerous diseases, including cancer, neurodegeneration, diabetes, and autoimmune diseases (5, 6). Accumulating evidence supports the importance of mTORC1 as an integrative hub for nutritional signaling; however, little is known about the regulation mechanism for specific downstream signaling molecules in the mTORC1 signaling pathway.

Transcription factor EB (TFEB) is the master transcription factor involved in lysosome biogenesis (7). The active mTORC1 directly phosphorylates TFEB, thereby suppressing nuclear translocation (8), while unphosphorylated TFEB migrates from the cytosol to the nucleus. TFEB promotes the gene expression of lysosomal proteins, thereby increasing the number of lysosomes. In a previous study, we observed that the nuclear translocation of TFEB markedly increased in Ragulator-deficient macrophages, although they retained half the mTORC1 activity of wild-type macrophages (9, 10). This contrasting observation led us to hypothesize that Ragulator is an essential scaffold for mTORC1 in regulating the intracellular localization of TFEB. We hypothesized that the Ragulator complex not only activates mTORC1, but also induces the mTORC1-mediated phosphorylation of the downstream substrate, TFEB, *in situ* (Fig. 1A). To this end, we generated a unique Ragulator-deficient clone that possesses total mTORC1 activity. We observed that a more significant proportion of the TFEB protein translocated to the nucleus in the Ragulator-deficient clone, despite retaining total mTORC1 activity. We also observed a tenfold increase in the number of lysosomes in the Ragulator-deficient clone compared with the control cells. These data indicate that the Ragulator complex not only acts as a scaffold for the activation of mTORC1 but also contributes to the phosphorylation of TFEB by mTORC1.

## Results

### Generation of Ragulator-deficient clone with total mTORC1 activity

The Ragulator protein complex comprises five proteins, namely Lamtor1, Lamtor2, Lamtor3, Lamtor4, and Lamtor5 (11). The data from our previous study demonstrated that the loss of Lamtor1 results in the loss of the four other proteins of the Ragulator complex (10). We generated a Ragulator-deficient RAW264.7 clone using a lentiviral vector expressing a short hairpin RNA (shRNA) to target Lamtor1. We subsequently obtained a clone that completely lacked Lamtor1

\* For correspondence: Tetsuya Kimura, [tetsuyakimura@biken.osaka-u.ac.jp](mailto:tetsuyakimura@biken.osaka-u.ac.jp).

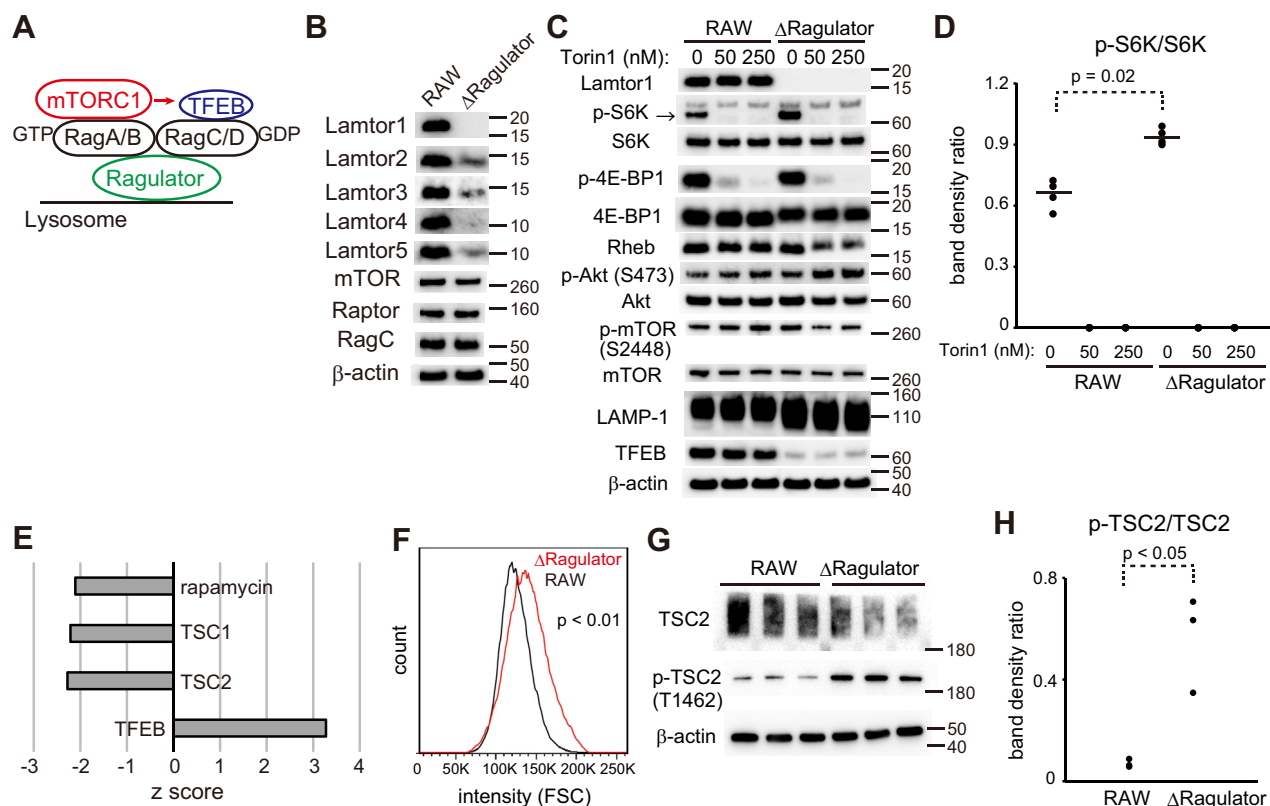


**Figure 1. Generation of Ragulator-deficient clone with total mTORC1 activity.** *A*, schematic representation of the findings of this study, depicting the phosphorylation of the TFEB substrate by mTORC1 bound to the Ragulator-Rag scaffold. *B*, the results of Western blotting studies on ΔRagulator and parental RAW264.7 cells. Lamtor1, Lamtor2, Lamtor3, Lamtor4, and Lamtor5 are components of the Ragulator complex; β-actin served as the internal control; mTOR and Raptor are components of mTORC1; RagC is necessary for the docking of TFEB to Ragulator. *C*, representative result of Western blotting studies for determining the activity of mTORC1. The control RAW264.7 cells and ΔRagulator cells were cultured in nutrient-sufficient and serum-supplemented DMEM. The phosphorylation of S6K in these cells was abolished following treatment with the mTOR kinase inhibitor, Torin1, at the indicated concentrations for 1 h. *D*, the densities of the p-S6K and S6K bands in panel *C* were quantified. The ratio of densities of the p-S6K band to S6K band is shown. Four independent experiments were performed. Bars indicate the median. Statistical significance was calculated using Mann–Whitney U test. *E*, the results of Upstream Regulator Analysis, as determined using the web-based software, Ingenuity Pathway Analysis. The pathways with z scores less than –2 are significantly inactivated in the ΔRagulator cells, compared to the RAW264.7 cells. The z score for the TFEB pathway was >2, which indicates that TFEB is significantly activated in the ΔRagulator cells than in the control RAW264.7 cells. *F*, the sizes of the ΔRagulator cells were larger than those of the parental RAW264.7 cells. The cell sizes of  $1 \times 10^4$  cells were estimated using flow cytometry. Statistical significance was calculated using Welch’s *t* test. *G*, Western blotting for determining the phosphorylation of TSC2. Control RAW264.7 cells and ΔRagulator cells were cultured in nutrient-sufficient and serum-supplemented DMEM. Three biological triplicates were examined. *H*, the densities of the p-TSC2 and the TSC2 bands in panel *G* were quantified. The ratio of densities of the p-TSC2 band to TSC2 band is shown. Statistical significance was calculated using the Mann–Whitney U test. mTORC1, mammalian target of rapamycin complex 1; TFEB transcription factor EB.

expression (Fig. 1B). The levels of the other Ragulator components, Lamtor2, Lamtor3, Lamtor4, and Lamtor5, also decreased in this clone (Fig. 1B, hereafter referred to ΔRagulator). The levels of the proteins of the mTOR signaling pathway, including mTOR, Raptor, RagC, Rheb, and Akt, were not affected by the Lamtor1 knockdown. The expression of these proteins in the ΔRagulator cells was similar to that of the parental RAW264.7 cells (Fig. 1, B and C). In order to determine the kinase activity of mTORC1 in the ΔRagulator cells, we determined the phosphorylation levels of p70 S6 kinase (S6K) and 4E-binding protein 1 (4E-BP1). Interestingly, the phosphorylation levels of S6K in the ΔRagulator cells were higher than those of the control RAW264.7 cells (Fig. 1, C and D). Following a brief treatment with the mTOR inhibitor, Torin1, the phosphorylation of S6K and 4E-BP1 was completely abolished in the cells. Therefore, the increase in the levels of these phosphorylated proteins indicated an increased mTORC1 activity in these cells (Fig. 1, C and D). In order to

confirm that ΔRagulator has enhanced mTORC1 activity, we performed gene expression microarray analyses and investigated the expression of the target genes of mTORC1. The results of upstream regulator analysis performed using the Ingenuity Pathway Analysis application suggested that the activity of mTORC1 increased in the ΔRagulator clone. Detailed analysis revealed that the z scores of the gene sets “rapamycin,” “TSC1,” and “TSC2,” all of which are mTORC1 suppressors, were significant negative, indicating an increased mTORC1 activity (Fig. 1E). Additionally, the sizes of the ΔRagulator cells were larger than those of the parental RAW264.7 cells, and this observation was consistent with the increased mTORC1 activity in the ΔRagulator cells (11) (Fig. 1F). We found that phosphorylation of TSC2 was increased in ΔRagulator cells (Fig. 1, G and H), which explains why mTORC1 activity was maintained in these cells. This finding was consistent with the result of upstream regulator analysis, which indicated the suppressed activity of the

negative *mTORC1* regulator TSC1/TSC2 complex (Fig. 1E). We therefore established a Ragulator-deficient clone in which the activity of *mTORC1* was higher than 100%.

**Nuclear translocation of TFEB occurs regardless of total *mTORC1* activity in  $\Delta$ Ragulator cells**

The  $\Delta$ Ragulator cells enabled us to investigate the role of the Ragulator complex as a scaffold for the phosphorylation of TFEB, in the absence of the kinase activity of *mTORC1*.

We observed that TFEB localized exclusively in the cytosol under nutrient-sufficient conditions in the control RAW264.7 cells (Fig. 2, A and B). More than half the quantity of TFEB translocated to the nucleus following amino acid starvation or treatment with Torin1 (Fig. 2, A and B). In contrast, the nuclear localization of TFEB was markedly increased in the  $\Delta$ Ragulator cells cultured in a nutrition-sufficient medium (Fig. 2, A and B). The nuclear/cytosolic ratio of TFEB in the  $\Delta$ Ragulator cells grown under nutrition-sufficient conditions was higher than that of the control

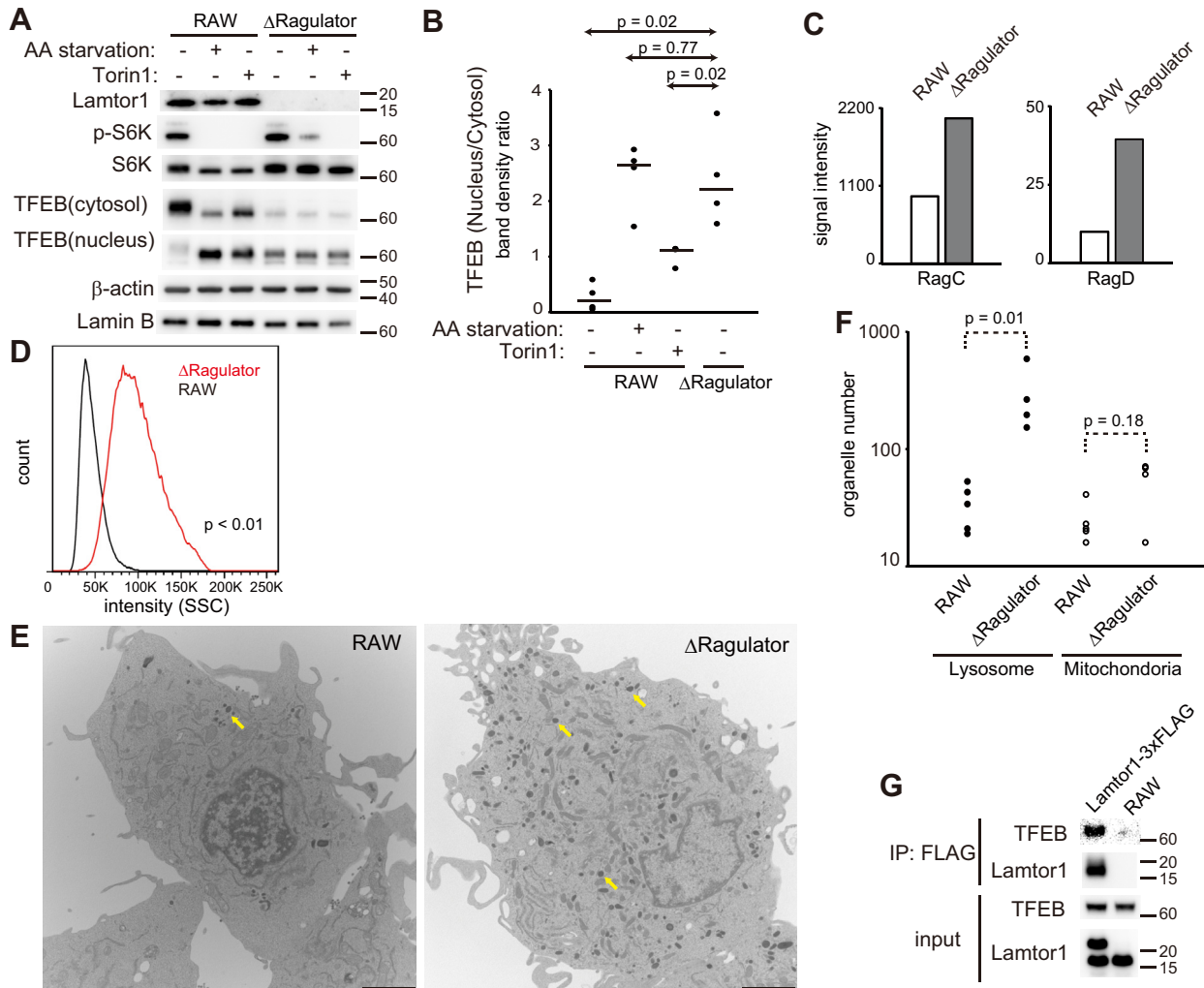


**Figure 2. Nuclear translocation of TFEB occurs in Ragulator-deficient cells, regardless of total *mTORC1* activity.** A, representative result of Western blotting for determining the activity of *mTORC1* and subcellular distribution of TFEB. The nuclear translocation of TFEB increased in the  $\Delta$ Ragulator and RAW264.7 cells after 1 h of amino acid starvation and treatment with 250 nM of Torin1. The internal controls for the cytosolic and nuclear fractions were  $\beta$ -actin and Lamin B, respectively. The quantities of S6K, phospho-S6K, and Lamtor1 were determined from the cytosolic fraction, which contained the lysosomes. B, the density of the TFEB band in panel A was quantified. The ratio of nuclear to cytosolic TFEB is shown. Four independent experiments were performed. Bars indicate the median. Statistical significance was calculated using the Mann-Whitney U test. C, gene expression microarray revealed that expression levels of *RagC* and *RagD* genes in  $\Delta$ Ragulator cells were higher than those in control RAW264.7 cells. D, the intensity of SSC for the  $\Delta$ Ragulator and RAW264.7 cells were obtained by flow cytometric analysis of  $1 \times 10^4$  cells. A high intensity of SSC is indicative of increased intracellular complexity, such as an increase in the numbers of organelles. Statistical significance was calculated using Welch's *t* test. E, the images obtained by transmission electron microscopy of  $\Delta$ Ragulator cells and parental RAW264.7 cells are depicted. The cells were cultured in nutrient-sufficient and serum-supplemented DMEM for 1 day, and then fixed immediately. The representative images of the cells obtained by transmission electron microscopy are provided. The yellow arrows indicate the lysosomes. The scale bar represents 2  $\mu$ m. F, the number of lysosomes and mitochondria in the cells were quantified from the images obtained by electron microscopy. Each of the dots represents a single cell. Statistical significance was calculated using the Mann-Whitney U test. G, immunoprecipitation using the anti-FLAG antibody. A RAW264.7 clone that stably expressed the Lamtor1-3xFLAG protein was used for the immunoprecipitation studies, along with the parental RAW264.7 cells. The high-molecular-weight Lamtor1 protein in the input sample was Lamtor1-3xFLAG, while the low-molecular-weight band represents the endogenous Lamtor1. The results proved the occurrence of a mechanistic association between TFEB and Lamtor1. DMEM, Dulbecco's modified Eagle's medium; *mTORC1*, mammalian target of rapamycin complex 1; TFEB transcription factor EB.

## ACCELERATED COMMUNICATION: mTORC1 essentially requires Ragulator to regulate TFEB

RAW264.7 cells treated with Torin1. It was comparable with RAW264.7 cells grown under amino-acid-starved conditions (Fig. 2B). We performed a transcriptomic analysis for investigating the transcriptional activity of TFEB in the  $\Delta$ Ragulator cells. The z score of the “TFEB” gene set, determined by upstream regulator analysis, was significantly positive, which indicated that the activity of TFEB is higher in  $\Delta$ Ragulator cells than in RAW264.7 cells (Fig. 1E). Activation of TFEB increases the expression of *RagC* and *RagD* genes to promote mTORC1 activation (12). Consistent with the previous finding, transcription levels of *RagC* and *RagD* genes increased in  $\Delta$ Ragulator cells, compared with RAW264.7 cells (Fig. 2C). It may also explain why mTORC1 activity was maintained in  $\Delta$ Ragulator cells. We next examined the lysosomal biogenesis in  $\Delta$ Ragulator cells. The results of the flow cytometric analyses revealed that the intensity of side scatter (SSC) in  $\Delta$ Ragulator cells was higher than that of the parental RAW264.7 cells, suggesting that  $\Delta$ Ragulator contained a significantly higher number of lysosomes than the control RAW264.7 cells (Fig. 2D). This was corroborated by the transmission electron microscopy results, which revealed that the  $\Delta$ Ragulator contained a higher number of lysosomes than the control cells (Fig. 2E). Subsequent quantification revealed that the number of lysosomes in the  $\Delta$ Ragulator cells was tenfold that of the parental RAW264.7 cells (Fig. 2F). Finally, the results of immunoprecipitation studies revealed that TFEB was mechanistically associated with Lamtor1 (Fig. 2G). It confirms that the Ragulator complex serves as a specific scaffold for TFEB.

### Discussion

In this study, we demonstrated that the Ragulator complex is essential for suppressing the nuclear translocation of TFEB. Previous studies have demonstrated that the nuclear translocation of TFEB increases in Lamtor1-knockout (9) and Rag GTPase-knockout cells (13). However, this phenomenon was attributed to the reduction in mTORC1 activity in these knockout cells. A recent study revealed that phosphorylation of TFEB by active mTORC1 essentially requires amino acids, active RagC/D, and RagC/D-activator folliculin (FLCN); in contrast, only TSC-Rheb-mTORC1 axis activation is required for S6K and 4E-BP1 phosphorylation (14). In order to elucidate the role of the amino acid sensing machinery Ragulator complex in the regulation of TFEB localization, we established a unique  $\Delta$ Ragulator clone of RAW264.7 cells. Using the  $\Delta$ Ragulator clone, we demonstrated that a fully active mTORC1 is not sufficient for regulating the nuclear translocation of TFEB. Therefore, in addition to the previously known role of the Ragulator complex as a lysosomal scaffold for the activation of mTORC1 (15), we identified that the Ragulator complex functions as a specific scaffold for the mTORC1-mediated phosphorylation of TFEB. Integrating our findings with the previous report (14), we propose a model in which the Ragulator-RagC/D complex is the essential scaffold for the phosphorylation of TFEB by activated mTORC1 (Fig. 1A).

Our findings suggest that the Ragulator complex is an excellent target for the treatment of lysosomal storage diseases (LSDs). In LSDs, the mutation of lysosomal enzymes results in the accumulation of substrates in the lysosome (16). The aberrant accumulation of metabolites leads to the disruption of several lysosomal functions. Recently, researchers have proposed that LSDs can be treated by inducing the activation of TFEB (16, 17). The activation of TFEB ameliorates lysosomal abnormalities in LSDs *via* two mechanisms. First, TFEB increases the expression of lysosomal proteins, which helps overcome the reduction in enzymatic activity. The second mechanism involves the induction of lysosomal exocytosis by TFEB, which results in the excretion of lysosomal contents into the extracellular space. Recent studies have demonstrated that trehalose moderately increases TFEB activity during the treatment of murine models of LSDs (18, 19). In this study, we observed a marked increase in the nuclear translocation of TFEB and a tenfold increase in the number of lysosomes in the Ragulator-deficient clone,  $\Delta$ Ragulator, compared with that of the control cells. Therefore, molecules that mechanistically interfere with the endogenous Ragulator-RagC/D-TFEB interactions can serve as novel therapeutic agents for LSDs, by inducing the nuclear translocation of TFEB and increasing the number of lysosomes in LSDs.

In conclusion, the results of this study demonstrated that the Ragulator complex functions as a substrate-specific scaffold for mTORC1 and regulates the nuclear translocation of TFEB.

### Experimental procedures

#### Generation of $\Delta$ Ragulator Lamtor1-knockdown clone

RAW264.7 cells were purchased from ATCC. The cells were cultured in Dulbecco's modified Eagle's medium (DMEM, #08458-45, Nacalai Tesque) supplemented with 10% fetal bovine serum and 100 mg/ml penicillin-streptomycin. After two passages, the RAW264.7 cells were transfected with a commercial lentiviral vector expressing an shRNA targeting Lamtor1 (sc-108727-V, Santa Cruz Biotechnology). The lentiviral vector was a mixture of two vectors targeting the murine Lamtor1 mRNA. After 2 days of vector infection, the cells were cloned using the limiting dilution method. The clones that lacked Lamtor1 were screened by Western blotting.

#### Generation of stable Lamtor1-3 $\times$ FLAG expressing clone

A plasmid vector encoding Lamtor1-3 $\times$ FLAG was constructed using the C57BL/6j mouse *Lamtor1* cDNA and p3 $\times$ FLAG-CMV-14 plasmid (Sigma-Aldrich). The Lamtor1-3 $\times$ FLAG sequence was confirmed by Sanger sequencing. The plasmid vector was introduced into RAW264.7 cells using the FuGENE HD Transfection Reagent (Promega), according to the manufacturer's protocol. The stable clones were selected using G418 (#ant-gn-1, InvivoGen), and the limiting dilution method was used for subsequent cloning. The clones that expressed the highest amount of Lamtor1-3 $\times$ FLAG were selected by Western blotting.

### Preparation of cell lysate and Western blotting

The whole cell lysates were prepared using lysis buffer A (50 mM Tris-HCl [pH 7.4], 150 mM NaCl, 1 mM EDTA, 5% glycerol, 2% n-octyl- $\beta$ -D-glucopyranoside, and 1% Nonidet P-40) as previously reported (20). We used NE-PER Nuclear and Cytoplasmic Extraction Reagents (#78833, Thermo Fisher Scientific) for preparing the cytosolic and nuclear fractions. Successful fractionation using this reagent has been confirmed in a previous report (9). For Western blotting, the reduced protein samples for SDS-PAGE were prepared by boiling 1:1 mixtures of cell lysates and 2 $\times$  Laemmli sample buffer (#1610737, Bio-Rad Laboratories) containing 2-mercaptoethanol. For Western blotting, the antibodies against S6K (#2708), p-S6K (T389, #9234), Akt (#4691), p-Akt (Ser473, #4060), 4E-BP1 (#9644), p-4E-BP1 (#2855), Lamtor1 (#8975), Lamtor2 (#8145), Lamtor3 (#8168), Lamtor4 (#12284), Lamtor5 (#14633), mTOR (#2983), p-mTOR (Ser2448, #5536), Raptor (#2280), RagC (#9480), Rheb (#13879), TSC2 (#4308), and p-TSC2 (Thr1462, #3617) were purchased from Cell Signaling Technology; while the antibodies against Lamin B (sc-6216), LAMP-1(clone 1D4B) and  $\beta$ -actin (clone AC-15) were purchased from Santa Cruz Biotechnology. The antibody against TFEB (A303-673A) was purchased from Bethyl Laboratories. The horseradish-peroxidase-conjugated anti-rabbit and anti-mouse IgG antibodies were purchased from GE Healthcare.

### Immunoprecipitation studies

The cells of the stable Lamtor1-3 $\times$ FLAG clone were harvested and lysed with buffer previously described (13). Briefly, the lysis buffer consisted of 25 mM HEPES (pH 7.4), 150 mM NaCl, 5 mM EDTA, and 1% Triton X-100. After 30 min of incubation on ice, the cells were mechanically broken and subsequently centrifuged at 16,000g for 10 min at 4 °C. The supernatant was immunoprecipitated at 4 °C, 30 min on a rotary shaker, using anti-DDDDK-tag mAb-magnetic agarose (M185-10, Medical & Biological Laboratories) for immunoprecipitation. After washing four times with Tris-buffered saline (50 mM Tris-HCl, 150 mM NaCl, pH 7.5), elution was performed with 8 M urea buffer by shaking at 37 °C for 10 min. For Western blotting, a 1:1 mixture of the eluted sample and 2 $\times$  Laemmli sample buffer (Bio-Rad Laboratories) containing 2-mercaptoethanol was prepared, and the mixture was boiled for 5 min at 95 °C.

### Amino acid starvation

Amino-acid-free DMEM (048-33575, Fujifilm) was used for amino acid starvation. DMEM (#08458-45, Nacalai Tesque) was used as the control culture medium in the control setup. Fetal calf serum was not added to either the control or starvation media for the amino acid starvation experiments.

### RNA extraction and gene expression microarray analysis

The total RNA was extracted from the  $\Delta$ Ragulator and control RAW264.7 cells, using the RNeasy Mini kit (#74104; QIAGEN). For microarray analysis, 200 ng of the total RNA

was reverse-transcribed into double-stranded cDNA using AffinityScript multiple temperature reverse transcriptase (Agilent Technologies). The resulting complementary RNAs were labeled with cyanine-3 (PerkinElmer) using a Low Input Quick-Amp Labeling kit (Agilent Technologies). The hybridization experiments were performed using Agilent Whole Mouse Genome Microarray 4 $\times$ 44K ver.2 kit (design ID 026655). The GeneSpring GX software, version 14.9.1, from Agilent, was used for calculations.

### Transmission electron microscopy

The cells were cultured on a polystyrene Cell Desk cover-slip (Sumitomo Bakelite) and fixed with 2% formaldehyde and 2.5% glutaraldehyde in 0.1 M sodium phosphate buffer (pH 7.4). The cells were then washed thrice for 5 min in the same buffer and subsequently in 0.1 M sodium phosphate buffer (pH 7.4) containing 1% osmium tetroxide and 1% potassium ferrocyanide for 1 h. The cells were then dehydrated in a graded ethanol series and embedded in Epon 812 (TAAB Laboratories Equipment). Ultra-thin sections (80 nm) of the specimens were stained with saturated uranyl acetate and lead citrate solutions. The electron micrographs were obtained using a JEM-1400 Plus transmission electron microscope (JEOL).

### Flow cytometry

The cells were analyzed using a FACSCanto II system (Becton, Dickinson and Company). The intensities of forward scatter (FSC) and SSC, which are indicative of cell size and intracellular complexity, respectively, were determined using a blue laser.

### Data availability

The microarray data have been deposited in NCBI-GEO under accession number GSE171357.

---

**Acknowledgments**—The authors acknowledge Ms Hiroko Ohmori of the Central Laboratory of WPI Immunology Frontier Research Center, Osaka University, for assisting in the studies on electron microscopy. This study was supported by the JSPS KAKENHI Grant-in-aid for Young Scientists (grant number: 18K16200), Visionary Research Grant from Takeda Science Foundation, Research Grant in the Natural Sciences (young scientist grant) from the Mitsubishi Foundation, and a grant from the Mochida Memorial Foundation for Medical and Pharmaceutical Research.

**Author contributions**—T. K. conceptualization; D. O. formal analysis; T. K. funding acquisition; T. K., Y. H., and D. O. investigation; T. K. methodology; T. K. project administration; S. N. and M. O. resources; M. O. supervision; T. K. visualization; T. K. writing—original draft

**Conflict of interest**—The authors declare that they have no conflicts of interest with the contents of this article.

**Abbreviations**—The abbreviations used are: 4E-BP1, 4E-binding protein 1; LSDs, lysosomal storage diseases; mTORC1, mammalian

target of rapamycin complex 1; S6K, S6 kinase; TFEB, transcription factor EB.

## References

1. Liu, G. Y., and Sabatini, D. M. (2020) mTOR at the nexus of nutrition, growth, ageing and disease. *Nat. Rev. Mol. Cell. Biol.* **21**, 183–203
2. Peterson, T. R., Sengupta, S. S., Harris, T. E., Carmack, A. E., Kang, S. A., Balderas, E., Guertin, D. A., Madden, K. L., Carpenter, A. E., Finck, B. N., and Sabatini, D. M. (2011) mTOR complex 1 regulates lipin 1 localization to control the SREBP pathway. *Cell* **146**, 408–420
3. Ben-Sahra, I., Hoxhaj, G., Ricoult, S. J. H., Asara, J. M., and Manning, B. D. (2016) mTORC1 induces purine synthesis through control of the mitochondrial tetrahydrofolate cycle. *Science* **351**, 728–733
4. Ben-Sahra, I., Howell, J. J., Asara, J. M., and Manning, B. D. (2013) Stimulation of de novo pyrimidine synthesis by growth signaling through mTOR and S6K1. *Science* **339**, 1323–1328
5. Efeyan, A., Zoncu, R., and Sabatini, D. M. (2012) Amino acids and mTORC1: From lysosomes to disease. *Trends Mol. Med.* **18**, 524–533
6. Jung, S., Gámez-Díaz, L., Proietti, M., and Grimbacher, B. (2018) “Immune TOR-opathies,” a novel disease entity in clinical immunology. *Front. Immunol.* **9**, 966
7. Sardiello, M., Palmieri, M., di Ronza, A., Medina, D. L., Valenza, M., Gennarino, V. A., Di Malta, C., Donaudy, F., Embrione, V., Polishchuk, R. S., Banfi, S., Parenti, G., Cattaneo, E., and Ballabio, A. (2009) A gene network regulating lysosomal biogenesis and function. *Science* **325**, 473–477
8. Settembre, C., Zoncu, R., Medina, D. L., Vetrini, F., Erdin, S., Erdin, S., Huynh, T., Ferron, M., Karsenty, G., Vellard, M. C., Facchinetti, V., Sabatini, D. M., and Ballabio, A. (2012) A lysosome-to-nucleus signalling mechanism senses and regulates the lysosome *via* mTOR and TFEB: Self-regulation of the lysosome *via* mTOR and TFEB. *EMBO J.* **31**, 1095–1108
9. Hayama, Y., Kimura, T., Takeda, Y., Nada, S., Koyama, S., Takamatsu, H., Kang, S., Ito, D., Maeda, Y., Nishide, M., Nojima, S., Sarashina-Kida, H., Hosokawa, T., Kinehara, Y., Kato, Y., *et al.* (2018) Lysosomal protein Lamtor1 controls innate immune responses *via* nuclear translocation of transcription factor EB. *J. Immunol.* **200**, 3790–3800
10. Kimura, T., Nada, S., Takegahara, N., Okuno, T., Nojima, S., Kang, S., Ito, D., Morimoto, K., Hosokawa, T., Hayama, Y., Mitsui, Y., Sakurai, N., Sarashina-Kida, H., Nishide, M., Maeda, Y., *et al.* (2016) Polarization of M2 macrophages requires Lamtor1 that integrates cytokine and amino acid signals. *Nat. Commun.* **7**, 13130
11. Bar-Peled, L., Schweitzer, L. D., Zoncu, R., and Sabatini, D. M. (2012) Ragulator is a GEF for the Rag GTPases that signal amino acid levels to mTORC1. *Cell* **150**, 1196–1208
12. Di Malta, C., Siciliano, D., Calcagni, A., Monfregola, J., Punzi, S., Pastore, N., Eastes, A. N., Davis, O., De Cegli, R., Zampelli, A., Di Giovannantonio, L. G., Nusco, E., Platt, N., Guida, A., Ogmundsdottir, M. H., *et al.* (2017) Transcriptional activation of RagD GTPase controls mTORC1 and promotes cancer growth. *Science* **356**, 1188–1192
13. Martina, J. A., and Puertollano, R. (2013) Rag GTPases mediate amino acid-dependent recruitment of TFEB and MITF to lysosomes. *J. Cell Biol.* **200**, 475–491
14. Napolitano, G., Di Malta, C., Esposito, A., De Araujo, M. E. G., Pece, S., Bertalot, G., Matarese, M., Benedetti, V., Zampelli, A., Stasyk, T., Siciliano, D., Venuta, A., Cesana, M., Vilaro, C., Nusco, E., *et al.* (2020) A substrate-specific mTORC1 pathway underlies Birt–Hogg–Dubé syndrome. *Nature* **585**, 597–602
15. Sancak, Y., Bar-Peled, L., Zoncu, R., Markhard, A. L., Nada, S., and Sabatini, D. M. (2010) Ragulator-Rag complex targets mTORC1 to the lysosomal surface and is necessary for its activation by amino acids. *Cell* **141**, 290–303
16. Marques, A. R. A., and Saftig, P. (2019) Lysosomal storage disorders – challenges, concepts and avenues for therapy: Beyond rare diseases. *J. Cell Sci.* **132**, jcs221739
17. Spanpanato, C., Feeney, E., Li, L., Cardone, M., Lim, J., Annunziata, F., Zare, H., Polishchuk, R., Puertollano, R., Parenti, G., Ballabio, A., and Raben, N. (2013) Transcription factor EB (TFEB) is a new therapeutic target for Pompe disease. *EMBO Mol. Med.* **5**, 691–706
18. Lotfi, P., Tse, D. Y., Di Ronza, A., Seymour, M. L., Martano, G., Cooper, J. D., Pereira, F. A., Passafaro, M., Wu, S. M., and Sardiello, M. (2018) Trehalose reduces retinal degeneration, neuroinflammation and storage burden caused by a lysosomal hydrolase deficiency. *Autophagy* **14**, 1419–1434
19. Rusmini, P., Cortese, K., Crippa, V., Cristofani, R., Cicardi, M. E., Ferrari, V., Vezzoli, G., Tedesco, B., Meroni, M., Messi, E., Piccolella, M., Galbiati, M., Garrè, M., Morelli, E., Vaccari, T., *et al.* (2019) Trehalose induces autophagy *via* lysosomal-mediated TFEB activation in models of motoneuron degeneration. *Autophagy* **15**, 631–651
20. Nada, S., Hondo, A., Kasai, A., Koike, M., Saito, K., Uchiyama, Y., and Okada, M. (2009) The novel lipid raft adaptor p18 controls endosome dynamics by anchoring the MEK–ERK pathway to late endosomes. *EMBO J.* **28**, 477–489